Engineering and Technology Journal
Journal homepage: https://etj.uotechnology.edu.iq

Evaluation of PCL Electrospun Scaffolds Concentration on Metformin Hydrochloride Release Ratio

Saja A. Moosa [a], **Akram R. Jabur** [*a], **Emad S. Al- Hassani** [a], **Ahmed M. Al-Shammari** [b]

[a] Materials Engineering Dept, University of Technology, Baghdad, Iraq
[b] University of Mustansiriyah, Iraqi Center for Cancer and Medical Genetic Research
*Corresponding author Email: mailto:Akram.R.Jabur@uotechnology.edu.iq

HIGHLIGHTS

- Metformin Hydrochloride-Polycaprolactone (MH-PCL) nanofiber mats were synthesized using blend and emulsion electrospinning techniques.
- The MH drug release decreases with PCL concentration.
- The hydrophilic drug was encapsulated within the fiber core structure by the emulsion electrospinning technique.
- The drug-loaded electrospun scaffolds treat chronic diseases through controlled and long-term drug release.

ARTICLE INFO

Handling editor: Mustafa H. Al-Furaiji

Keywords:

Polycaprolactone; Metformin hydrochloride; Blend; Emulsion Electrospinning; Drug Delivery System.

ABSTRACT

The study investigates the effect of polycaprolactone (PCL) concentration on the metformin hydrochloride (MH) release ratio of electrospun nanofiber scaffolds. Blend and emulsion electrospinning are used to produce the scaffolds. The performance of nanofibrous scaffolds was evaluated by morphology (Field Emission Scanning Electron Microscopy, FESEM), chemical (Fourier Transform Infrared Spectroscopy, FTIR), thermal (Differential Scanning Calorimetry, DSC), wettability, porosity, mechanical tests, and in vitro drug release. The average fiber diameter ranged from (189.29-2893.93 nm) according to the FESEM results, and it increased with PCL concentration. The average fiber diameter of the electrospun scaffold, prepared by the blend method (259.64±6.1 nm), is lower than that of the electrospun scaffold produced by the emulsion method (487.45±22.53 nm). Melting points of all drug-loaded scaffolds were identical to those of pure PCL polymer. Compared with blend electrospun nanofibers, emulsion electrospun nanofibers showed a marked increase in hydrophilicity. The tensile strength indicated an improvement in the mechanical properties with a decrease in the average fiber diameter. Moreover, the results show that the release of Metformin hydrochloride decreases with the concentration of polycaprolactone. Total MH release from (5% w/v) PCL-MH fibrous scaffolds for three-week was 71.11 % and 93.91 % from the emulsion and blend methods, respectively. The drug release ratio is lower in emulsion electrospinning than in blend because the drug is encapsulated by polymer and surfactant, which improves control and long-term drug delivery system DDS.

1. Introduction

With the rapid advances in nanotechnology in recent years, incorporating bioactive components into polymer materials for controlled therapeutic release has become a vital field of research. Encapsulating bioactive ingredients in drug delivery systems (DDSs) is a valid way to protect these constituents from degradation in harsh environments, reduce side effects, improve solubility, achieve controlled release, and improve biocompatibility [1]. Fibers artificial spinning is a core part of today's bioinspired technology. It takes advantage of development in various techniques, including wet-spinning, dry-spinning, electrospinning, microfluidic spinning, direct drawing, and direct writing [2]. Electrospinning can be used to create a single-component polymer fibrous matrix with sub-micrometer diameters and composites [3,4]. The electrospinning method produces small diameter fibrils with linked pores in a non-woven matrix [5]. Many factors influence the shape and diameter of the resulting nanofibers. These factors have been classified into solution properties, process parameters, and environmental conditions [5]. Traditional electrospun nanofibrous drug delivery devices are fabricated by blending a drug/protein solution with a polymer solution [6]. The key disadvantages of the blend-electrospinning technique are the clearance and denaturation of drug/protein components and their acute burst release phenomena; this decreases the device's effective lifetime, particularly during the hydrophilic encapsulation therapeutics. Emulsion electrospinning is a novel technique for creating core-shell nanofibers that employ an emulsion. Emulsion electrospinning had used to encapsulate proteins, drugs, and growth factors into the inner core of

http://doi.org/10.30684/etj.2021.131990.1079
Received 30 October 2021; Accepted 07 December 2021; Available online 27 August 2022
2412-0758/University of Technology-Iraq, Baghdad, Iraq

the nanofibers [7,8]. Millions worldwide suffer from chronic cardiovascular illnesses such as high blood pressure, blood glucose, and cholesterol. Metformin hydrochloride (MH) is one medication used to treat chronic disorders [9]. Metformin hydrochloride (MH), also known as N, N-dimethyl imidodicarbonimidic diamide hydrochloride, is an oral antihyperglycemic of the biguanide family that improves glucose tolerance in type 2 diabetic patients by lowering both baseline and postprandial plasma glucose. Metformin reduces hepatic glucose synthesis, decreases intestinal glucose absorption, and raises insulin sensitivity by increasing peripheral glucose uptake and utilization [10,11]. Thus, our work demonstrates the potential of this novel scaffolding drug delivery system for cardiovascular tissue regeneration loaded with medication for sustained and controlled release. It involves an investigation of the effect of PCL concentration of scaffolds produced by blend and emulsion electrospinning.

2. Materials and Methods

2. 1 Materials

The Biodegradable polymer polycaprolactone (PCL) (average Mn 80000, was obtained from Sigma-Aldrich), Metformin hydrochloride (MH) was purchased from Merck, France, Sorbitan monooleate was purchased from HIMEDIA (Span 80, Molecular weight: 428.62g/mol), methylene chloride (MC) from alpha chemical (Assay:99.5%, Molecular weight: 84.93 g/mol), and N, N dimethylformamide (DMF) Central Drug House (P) limited company Corp. office (Assay:99.5%, Molecular weight: g/mol).

2. 2 Fabrication of PCL and Metformin-Loaded PCL Nanofibres

In the oil phase preparation, Polycaprolactone (5, 10, and 15 % w/v) was dissolved in MC with 1% Span 80 (v/v) to obtain the polymer solution. At ambient temperature, the polymer solution was stirred for three hours. Metformin hydrochloride concentration (5wt%) dissolved in water (water phase). To provide a drug-polymer suspension, droplets of the drug solution were further to the polymer solution. The drug-polymer ratio was kept constant in MH-PCL Nano-fibers (1:50) [12]. The equivalent amount of metformin incorporated with PCL in blend and emulsion electrospinning PCL Nanofibers had produced in their pure state. Table 1 provides further information about solvent systems. A bio-electrospinning/electrospray system (ESB-200) nano NC was used for electrospinning. A 16Kv voltage, a rate of 2 mL/h, and a needle-collector distance of 150 mm had used for the electrospinning polymer solution. Electrospun fibers had gathered on an electrically grounded Al foil. A drum collector was employed (speed 300 rpm). The electrospinning had done under ambient conditions.

Table1: Formula for preparation of scaffolds

Scaffold	Solvent
5% (w/v) PCL	MC:DMF(80: 20)
5% (w/v) PCL- 5% (wt.) MH/ blend	MC:DMF (80:20)
5% (w/v) PCL- 1% (v/v) span 80- 5% (wt.) MH/ emulsion	MC
10% (w/v) PCL	MC:DMF (80:20)
10% (w/v) PCL- 5% (wt.) MH/ blend	MC:DMF (80:20)
10% (w/v) PCL- 1% (v/v) span 80- 5% (wt.) MH/ emulsion	MC
15% (w/v) PCL	MC:DMF (80:20)
15% (w/v) PCL- 5% (wt.) MH/ blend	MC:DMF (80:20)
15% (w/v) PCL- 1% (v/v) span 80- 5% (wt.) MH/ emulsion	MC

2. 3 Characterization

2.3. 1 The morphology of Nano-fibers

A MIRA3-XMU microscope was used to acquire field emission scanning electron microscopy FESEM images. A thin layer of gold (~10 nm) was deposited into electrical links and allowed imaging by sputtering for 10 minutes before the analysis. The fiber diameters were analyzed using the AutoCAD2017 program.

2.3. 2 Infrared spectroscopy

FTIR (BRUKER, TENSOR-27) analyzed the chemical groups before and after drug loading.

2.3. 3 Differential scanning calorimetry (DSC)

(131 EVO-SETARAM) was used to determine the thermal properties of the produced scaffolds. For this purpose, use a heating rate of 10°C/min, at a temperature range of 25°C to 250°C.

2.3. 4 Wettability

The contact angle between the scaffold surface and the surrounding air was determined using a goniometer (CAM 110, Germany). Five microliters of water were dropped onto each scaffold, and images were recorded after 0, 1, and 10 min.

2.3. 5 Porosity

The average porosity of the electrospun sample was measured by the liquid displacement technique [13]. The porosity of electrospun mats was calculated according to the following equation [13]:

$$\text{Porosity (\%)} = \frac{W_w - W_d}{W_w - W_1} \times 100 \quad (1)$$

Where W_d: dry weight, W_w: wet weight, and W_1: weight after scaffold immersed in ethanol for 5 min [13].

2.3. 6 Mechanical properties

A Mechanical Analyzer (Tinus Olsen, H50 KT Instrument) in tension mode (ASTM D-882-02) was used to evaluate the mechanical properties of the scaffolds before and after drug loading (tensile strength, MPa; and elongation-at-break, reported as a percentage) in tension mode. The electrospun nanofibers (100×10 mm in size) were cut, and measurements were performed at 25°C at a strain rate of 1 mm/min.

2.3. 7 In vitro drug release

2.3.7. 1 Instrument

Spectral absorption measurements were performed using a UV-Visible spectrophotometer (T80+ UV/VIS spectrometer, PG Instruments Ltd), double beams spectrophotometer with spectral bandwidth (2 nm), and ± 0.3 nm wavelength accuracy. The wavelength range (190-1100 nm), 10×10mm quartz cell.

2.3.7. 2 Selection of analytical wavelength

Appropriate 10µg/ml dilutions of the drug were made from the standard stock solution. The solution was scanned in the 190-1100 nm wavelength range to obtain its absorption spectra with zero-order spectroscopy, which was chosen for the drug analysis. The absorption was taken at 235 nm, which can be further used for analysis.

2.3.7. 3 Preparation of stock solution

100 milligram of metformin was weighed and dissolved in 100 mL of phosphate buffer solution (PBS) to obtain a solution containing 1000 µg/ml (Stock solution A). From this stock solution A, measure 5 ml, and put it in a 50 ml volumetric flask. PBS was used to get the volume to the required level, yielding a solution containing 100µg/ml (Stock solution B).

2.3.7. 4 Calibration curve for the metformin

Prepare solutions in the concentration range (2-10 µg/ml) of metformin stock solution B to obtain the metformin calibration curve, Figure (13, b).

2.3.7. 5 Analysis of metformin from scaffold

Approximately 50 mg of a drug-loaded electrospun scaffold was cut into small pieces, then immersed in a phosphate buffer solution (PH =7.4) and incubated at 37°C. At prearranged periods, the PBS had withdrawn from each specimen for study. For continued incubation, another 5 mL of fresh PBS was added. This repeated procedure had repeated for three weeks. The amount of drug released into PBS at each period was examined by measuring the UV absorbance of metformin. The cumulated drug release ratio was calculated by the following formula:

$$\frac{M_t}{M_\infty} \times 100 \quad (2)$$

Where M_∞ is the total amount of drugs incorporated theoretically into the electrospun scaffolds, and Mt is the number of drugs released at each period t (time). The samples at all periods were tracked in triplicate [14].

3. Results and Discussion

3. 1 FESEM Result

Figure (1. A, B) shows the FESEM image for the processed 5 % w/v PCL scaffold. It could see from this image that the low polymer concentration resulted in a small fiber diameter since the average fiber diameter was about 189.29 ± 4.92 nm, as illustrated in figure (1. C), which will provide the large surface area. Also, the FESEM image shows the presence of rounded beads with fibers and damaged fiber, which results from the breakup of jets in solutions with low viscosity and low solution conductivity, respectively [15]. On the other hand, as shown in Figure (1.D), the average pore size was around 656.61±22.75nm. The average fiber diameter of drug-loaded nanofibers produced by the blend method was slightly great but more uniform than pure polymeric nanofibers. Average fiber increase (although the drug increased the solution conductivity) could be due to an increase in the viscosity of polymer solutions as a result of solvent evaporation, as shown in figure (2. A, B, C,D). The average fiber diameter was 259.64 ±6.1nm whereas, the pore size was 1029.59 ±26.76 nm. The MH-loaded nanofibers via emulsion were a larger average fiber diameter 487.245±22.53nm, and the average pore size was 2024.78± 128.65 nm, figure (3,a-b-c-d). With the addition of DMF solvent to the solution, conductivity and constant dielectric increase, while surface tension and viscosity

decrease, as shown in figure (6, b) [16,17]. When the polymer solution has a low surface tension, it easily stretches the polymer jet and produces thinner nanofibers. Figures (1,4, and 5) depicts the morphology of pure 5% w/v PCL and 10 % w/v PCL and 15% w/v PCL scaffolds. The average size of the fibers had discovered to be between 189.29±4.92 nm, 486.92±9.88 nm, and 2893.93±353.76, respectively. The solution concentration strongly influences fiber size; when solution concentration increases, fiber size rises rapidly exponentially, as illustrated in figure (6. A) [18]. At a low PCL concentration (5 percent w/v), beads developed on the fibers straight segment with spindle-like morphology, figure (1, a). Uniform fibers had produced at higher PCL concentrations, figures (4, 5). The formation of beads at low concentrations indicated that entanglement polymer chains, which were associated with a viscoelastic force present in the polymer charged jet, were sufficient to keep the PCL jet from breaking into drops. However, it was insufficient to eliminate capillary instability on the charged jet. As a consequence, beads appear on the fibers. Alternatively, at elevated concentrations, there was sufficient molecular entanglement to prevent the creation of jet instability on a large enough scale to be seen, leading to the formation of bead-free fibers [18].

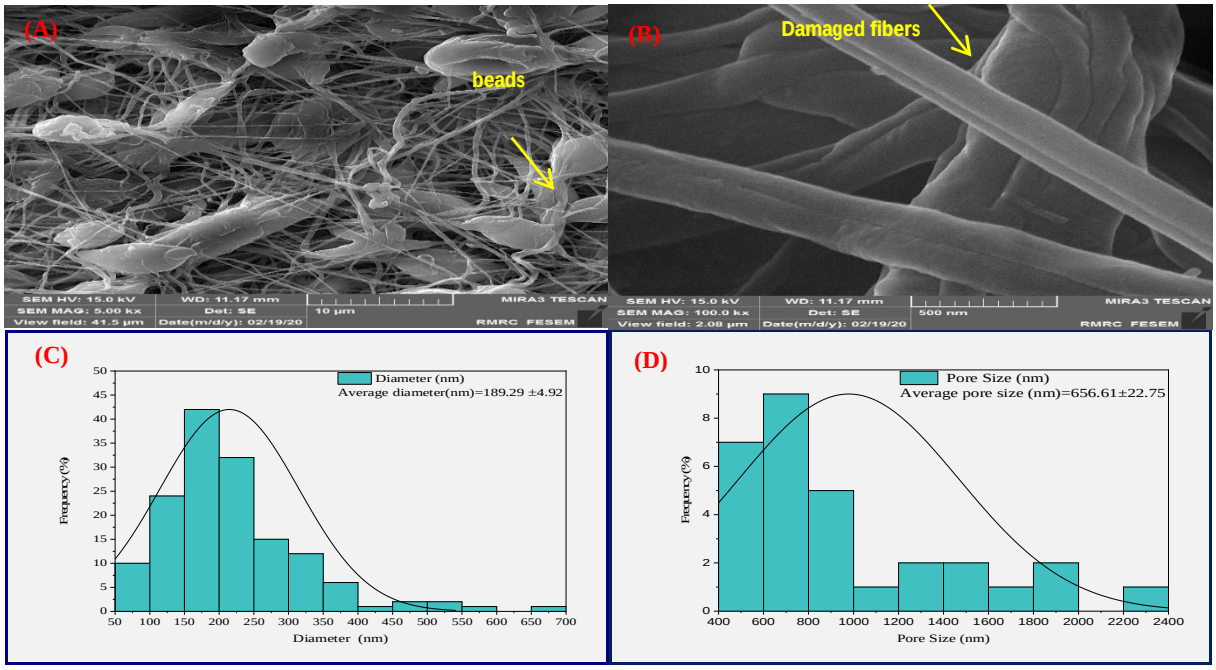

Figure 1: A. FESEM image of 5% (w/v) pure PCL with magnification 5 KX, B. magnification 100 KX, C. Average fiber diameter, and D. Average pore size

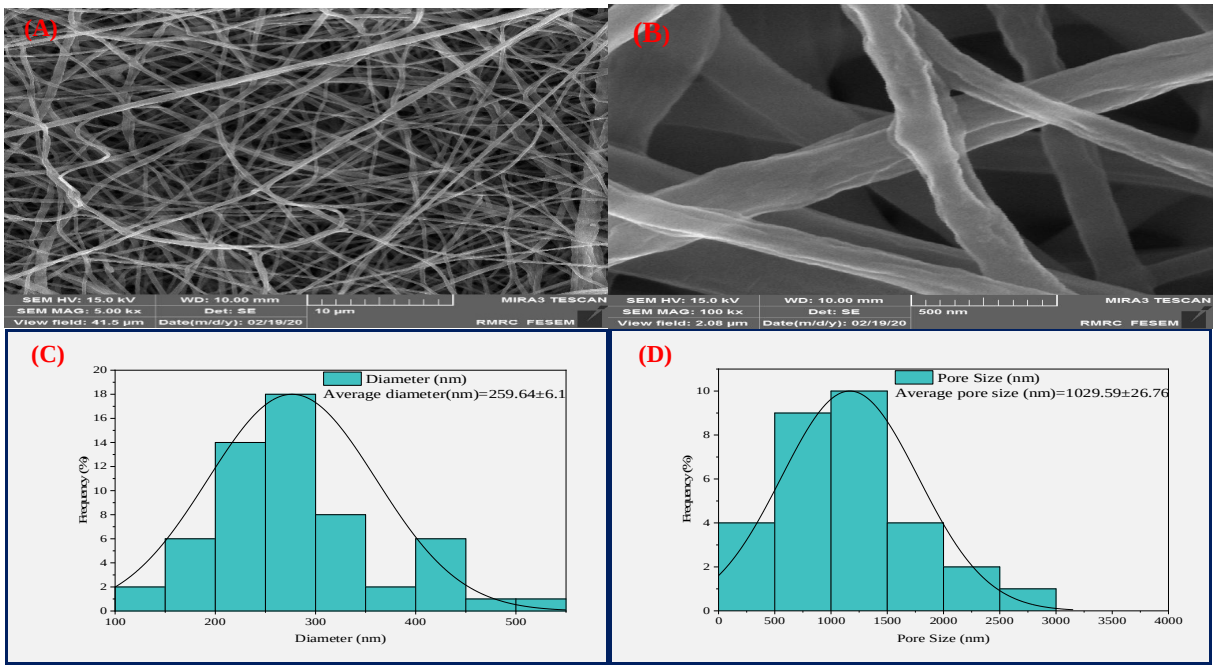

Figure 2: A. FESEM image of 5% (w/v) PCL-MH(5%wt.), blend method, with magnification 5 KX, B. magnification 100 KX, C. Average fiber diameter, and D. Average pore size

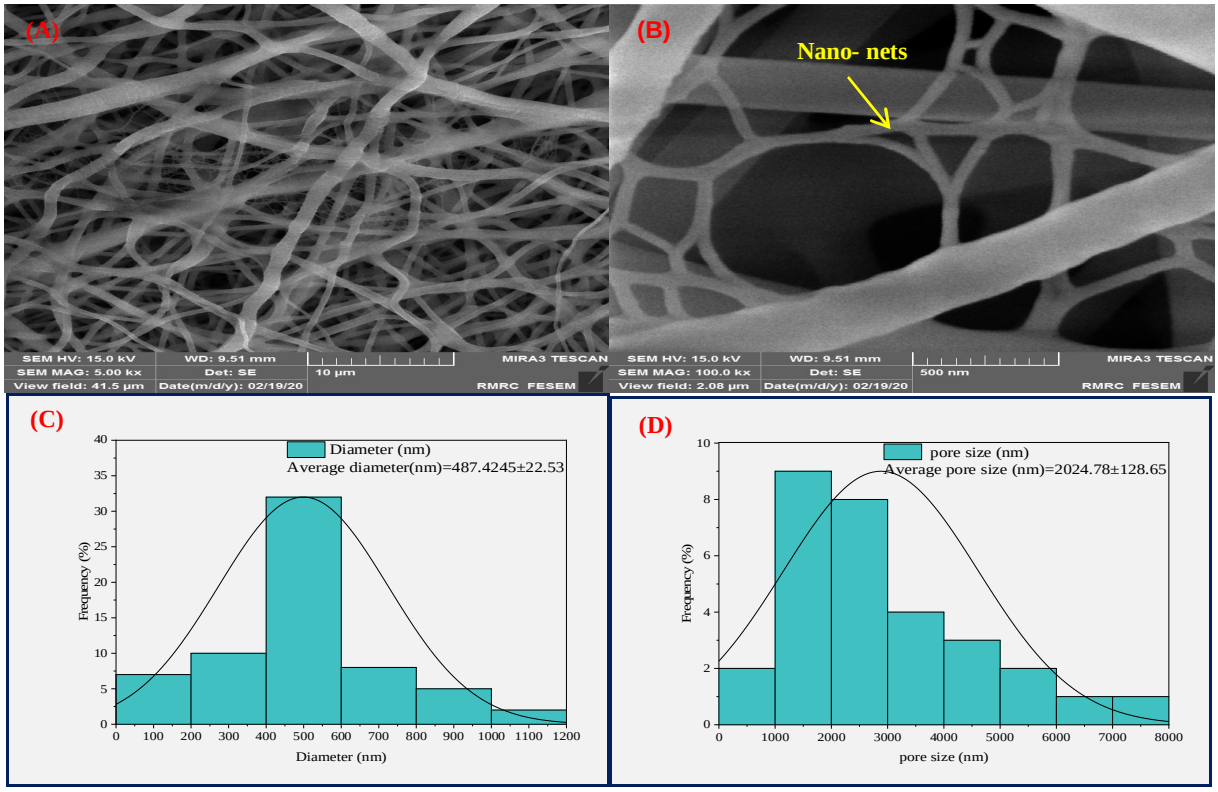

Figure 3: A. FESEM image of 5% (w/v) PCL-MH(5%wt.), emulsion method, with magnification 5 KX, B. magnification 100 KX, C. Average fiber diameter, and D. Average pore size

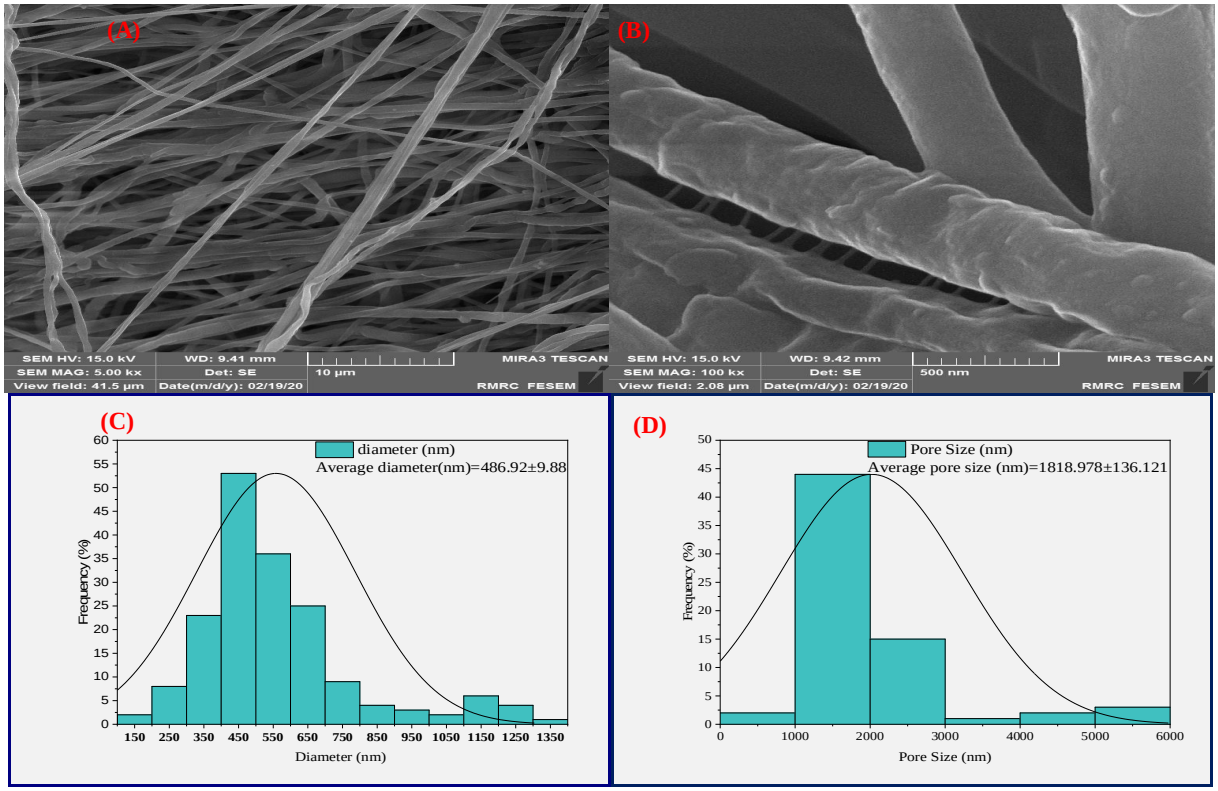

Figure 4: A. FESEM image of 10% (w/v) pure PCL with magnification 5 KX, B. magnification 100 KX, C. Average fiber diameter, and D. Average pore size

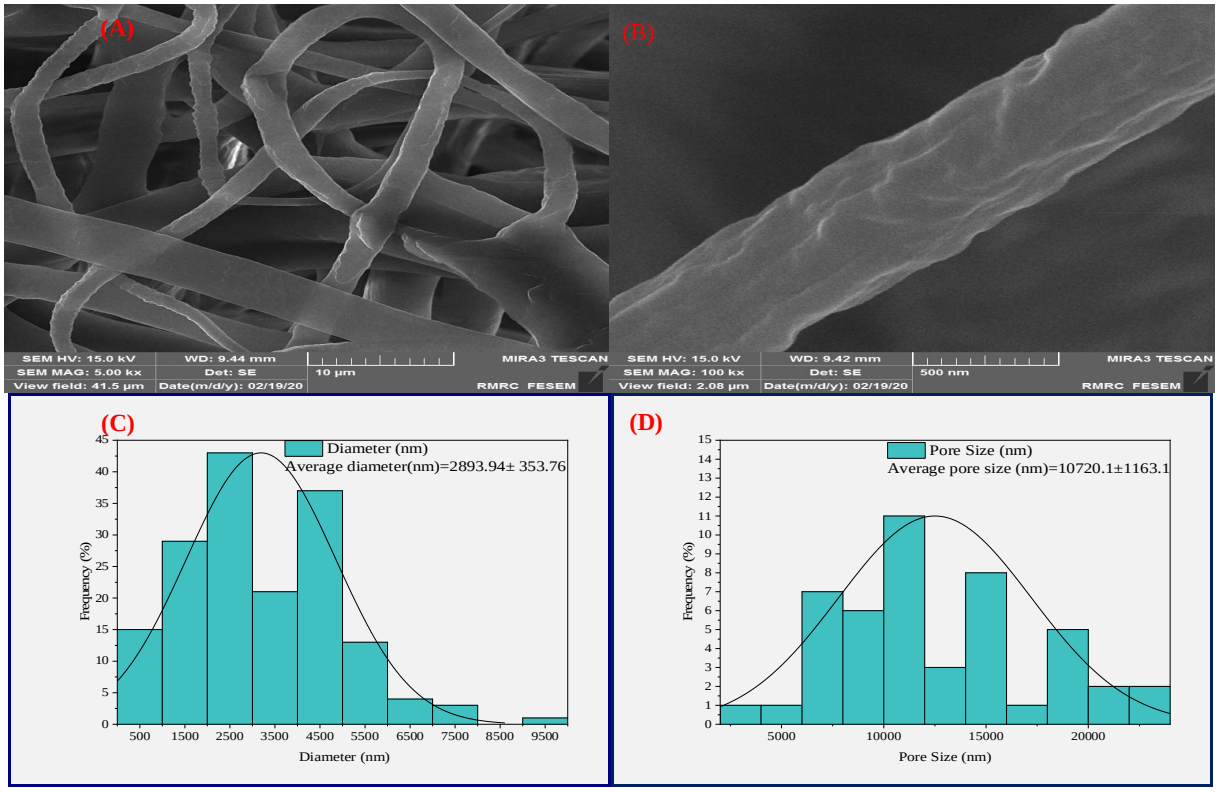

Figure 5: A. FESEM image of 15% (w/v) pure PCL with magnification 5 KX, B. magnification 100 KX, C. Average fiber diameter, and D. Average pore size

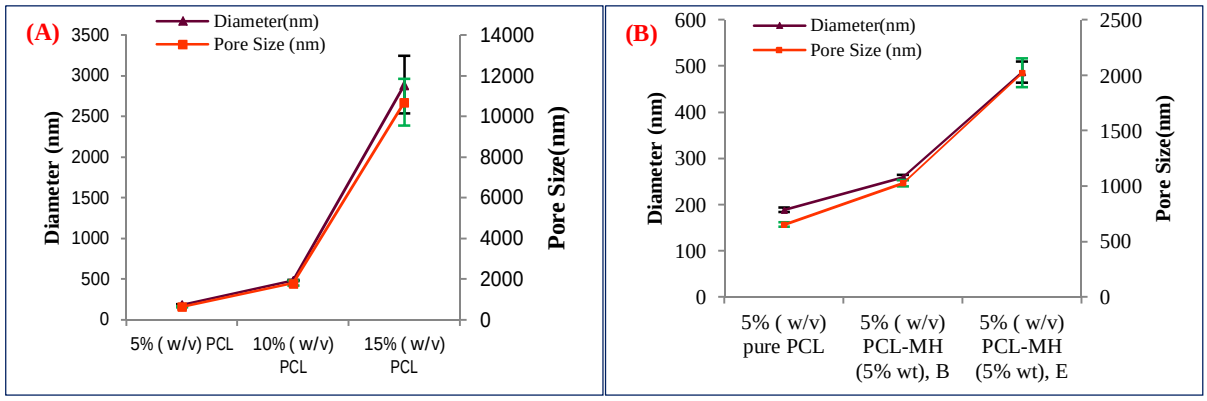

Figure 6: A. Plot of average fiber diameter and pore size vs. PCL concentration, B. Plot of average fiber diameter and pore size of pure PCL and MH loaded-PCL scaffolds.(B: Blend, E:Emulsion), error bar represent standard deviation

3. 2 FTIR Result

Figure 7 depicts the infrared spectra and vital absorption bands of materials. PCL spectrum displays characteristic peaks of C=O stretching vibrations (ester) at 1722.31 cm^{-1}, CH_2 bending modes at 1365, 1396, and 1470 cm^{-1}, and CH_2 asymmetric stretching at 2943.14 and symmetric stretching at 2865.4 cm^{-1} ((C-H) alkyl stretches). The C—O—C stretching vibrations yield peaks at 1045, 1106.61, and 1239 cm^{-1} [19], Figure 7 (black). FTIR spectrum of Metformin Hydrochloride, figure 7 (blue). The N-H stretching of the C=N–H group occurs in the region 3397.2-3090.4 cm^{-1}. The medium intensity bands at 3391, 3372 cm^{-1}, and 3293, 3153 cm^{-1} have been assigned to N-H asymmetric and symmetric stretching vibrations, respectively. Bands at 1563, and 1546 cm^{-1} are assigned for NH2 in-plane deformation vibrations. The bands of weak intensity at 937, 800, and 736 cm^{-1} are due to N-H wagging. Metformin biguanide has strong absorption bands at 1622 and 1584 cm^{-1} which are due to C=N stretching vibrations. The symmetric CH stretching vibration absorbs at 2885 - 2865 cm^{-1}. Bands at 2974 and 2816 cm^{-1} had assigned to CH_3 asymmetric and symmetric stretching vibrations of the methyl group, respectively [20] .The transmission peaks of drug-loaded nanofibers synthesized using various techniques are identical to those of pure PCL. The distinctive peaks of drugs were undetectable in the spectra of all drug-loaded nanofibers, with no additional absorption peaks appearing. These results showed no chemical interaction between metformin hydrochloride and polymers throughout the nanofiber production process, indicating the original components were not chemically changed.

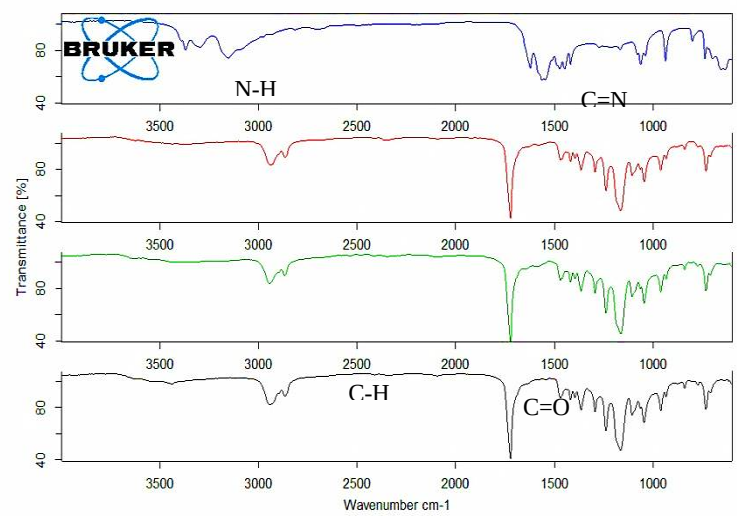

Figure 7: FTIR spectra of Pure PCL (black), metformin hydrochloride(blue), PCL-MH/Blend method (red), and PCL-MH/Emulsion method (green)

3. 3 DSC Results

Figure (8. a, b) shows DSC thermograms of several components, The crystalline character of metformin hydrochloride powders has to be demonstrated by a significant endothermic peak at 229 °C Jue Hu et al.[14] reported similar experimental results. The temperature at which pure PCL melts (Tm) 60°C. All drug-loaded scaffolds had identical melting points to pure PCL within a relatively limited temperature range. Blend electrospun scaffolds showed both polymer and drug peaks: 60°C and a tiny peak of 220°C corresponding to PCL and MH melting points, respectively. It does not reveal any phase change in MH and is in crystalline form. The low polymer-drug affinity of blend electrospun mats and metformin intrinsic physicochemical properties may explain the result. Unlike blend electrospun mat, MH encapsulated emulsion- electrospun scaffolds lack a drug endothermic peak.

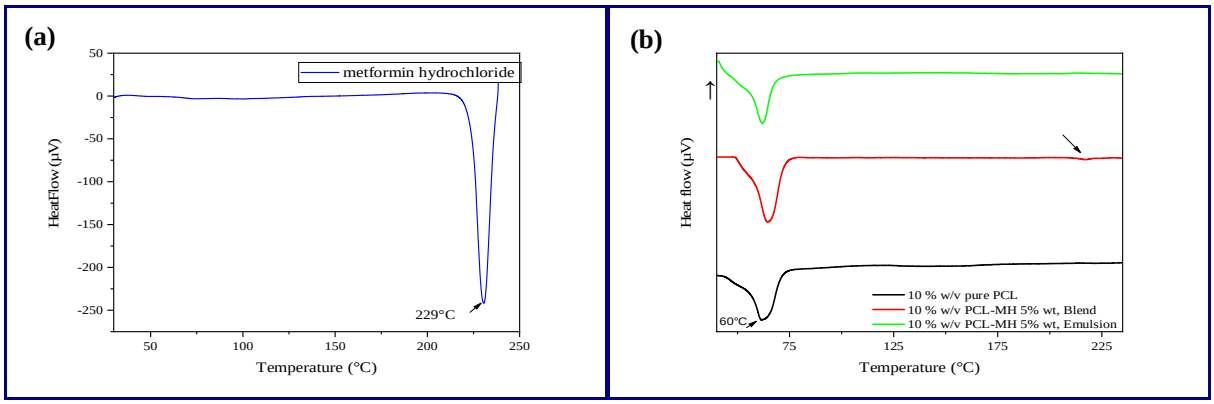

Figure 8: (a) DSC profiles of pure metformin hydrochloride drug, (b) DSC profiles of pure polymers and drug-loaded nanofibers

3. 4 Contact Angle Results

Pure PCL nanofibers are hydrophobic based on water contact angle values, as illustrated in figure (9). The average fiber diameter influences scaffold wettability because decreasing the fiber diameter makes the scaffold more hydrophobic [21]. Blend or emulsion electrospun drug-loaded nanofibers were significantly more hydrophilic than pure polymer nanofibers due to incorporating one or both the drug and the surfactant. Compared to blend electrospun nanofibers, emulsion electrospun nanofibers demonstrated significantly increased hydrophilicity. All of the scaffolds became hydrophilic over time, according to the results. The results mentioned above had explained by the fact that when surfactants Span 80 were added (through the emulsion process, figure (9, b)), a portion of the surfactants stabilized the water phase in the nanofibers' cores, while others transferred to the nanofibers' surfaces, increasing the hydrophobic polymer's wettability [22].

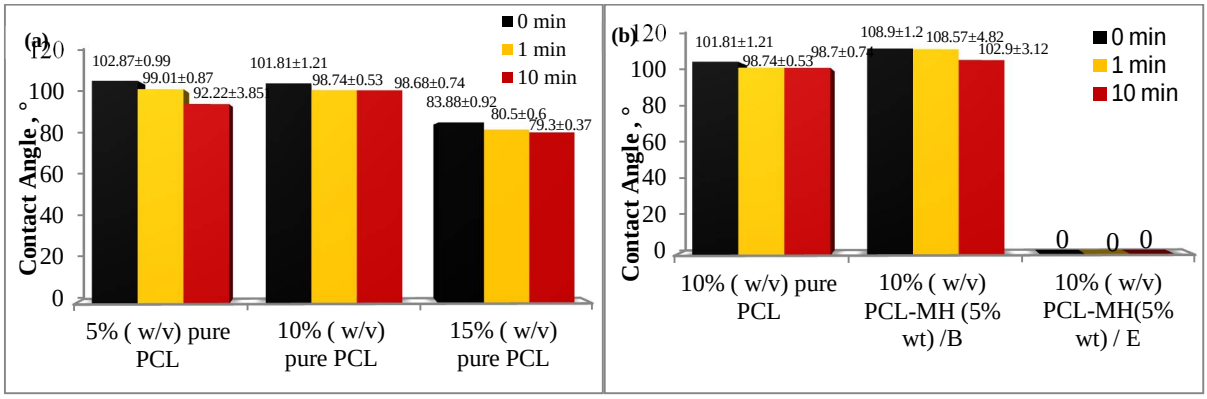

Figure 9: (a) Contact angle at different PCL concentrations, (b) Contact angle of pure polymers and drug-loaded nanofibers

3. 5 Porosity Results

The porosity test results are generally related to the average pore size of the produced scaffolds. Usually, a reduction in porosity had seen as the average pore size decreases, as shown in Figure (10, a). The porosity percentage of drug-encapsulated blend scaffolds differs somewhat from that of pure PCL scaffolds. The porosity of blend electrospun nanofiber with an average small pore size (1029.59±26.76nm) has decreased to (86.28%).

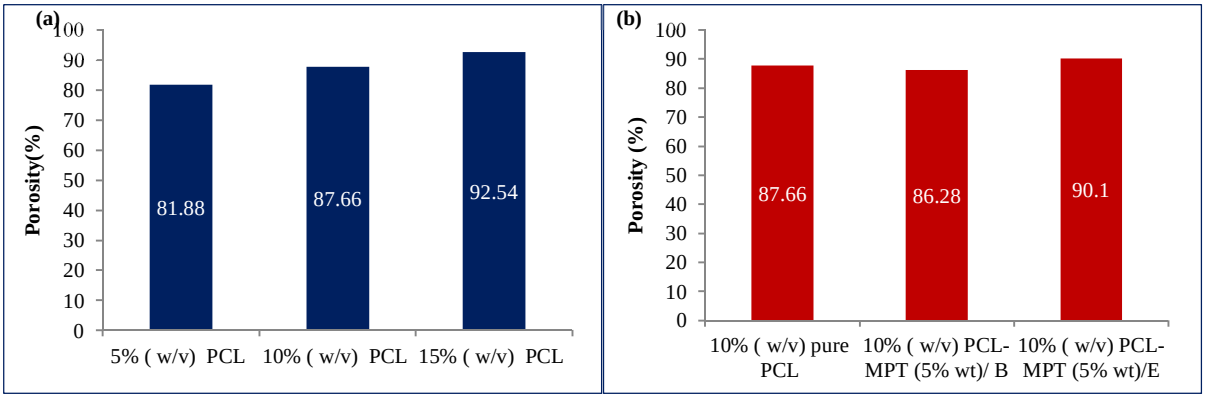

Figure 10: (a) Porosity vs. PCL concentration and (b) Porosity vs. pure polymers and drug-loaded nanofibers loaded nanofibers

3. 6 Tensile Test Result

The mechanical tests of PCL and PCL-drug-loaded nanofibers were performed under ambient conditions. Figure (11.a) shows stress-strain curve for pure PCL matrix at different concentrations (5,10, and 15 % (w/v)). The results of the tensile test indicated that mechanical properties improved with a decrease in the average fiber diameter due to the increased crystallinity and molecular orientation as the diameter of the fiber decreased [23]. The necking phenomenon does not occur in these electrospun fibers—Figure (11, b) the tensile strength and breakpoint vs. PCL concentration. As the fibers' diameter decreases, the fibers' strength increases, and the ductility of the fibers decrease [23].

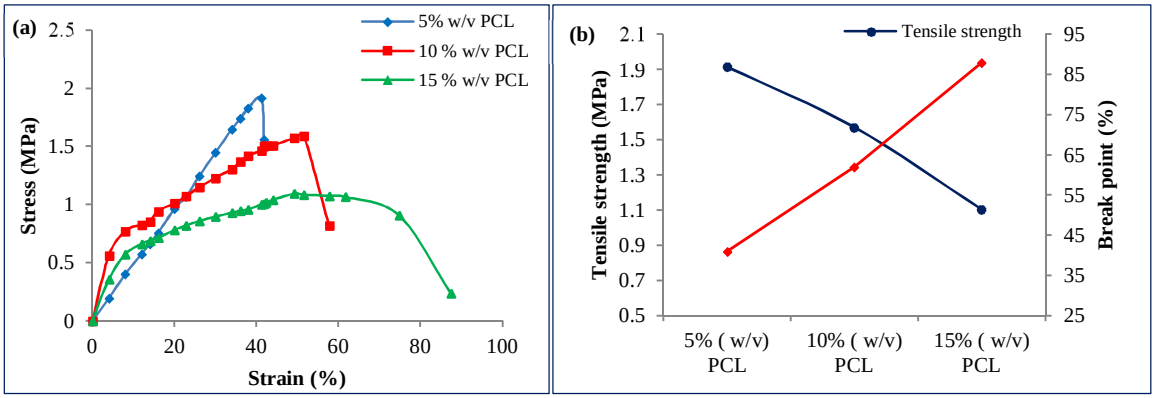

Figure 11: (a) Stress-strain curve of different concentrations of pure PCL scaffolds, (b) Tensile strength and breakpoint vs. PCL concentration

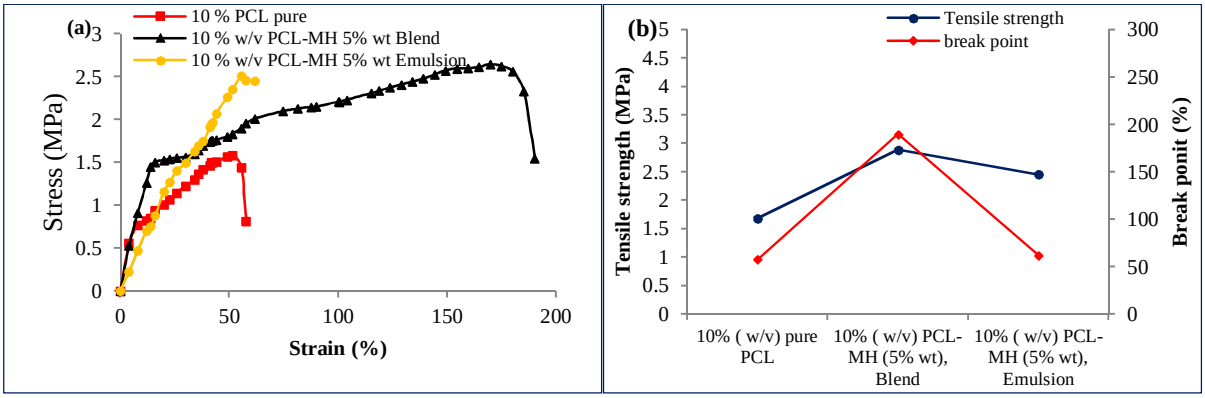

Figure 12: (a) Stress-strain curve of pure PCL and MH loaded-PCL scaffolds by blend and emulsion electrospinning, (b) Tensile strength and breakpoint of pure PCL and MH loaded-PCL scaffolds

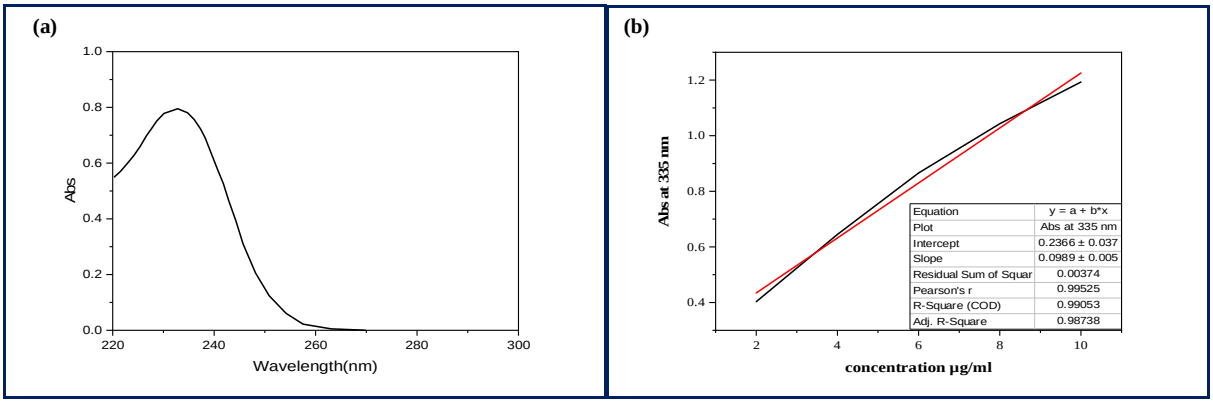

Figure 13: (a) UV Spectra of metformin hydrochloride, (b) Calibration curve of metformin hydrochloride drug

3. 7 In Vitro Drug Release Results

To evaluate the potential use of MH-PCL scaffolds as a drug delivery system, in vitro drug release profile of electrospun PCL scaffolds in PBS (pH 7.4) was studied. The UV-VIS spectra have the maximum band at 235nm, similar to experimental results reported by Y. Ankamma Chowdary et al. [24]. The standard solution of metformin hydrochloride (6µg/ml) was scanned in the range of 200-350 nm, with maxima centered at 235 nm (Figure 13, a). Figure (13, b) depicts the MH calibration curve in the range (of 2-10 µg/ml).

The cumulative release curve of MH/PCL electrospun scaffolds have shown in figure (14, a-c). The release profile of all MH-loaded fibrous scaffolds had divided into two stages. A burst release stage with a high quantity of MH within 12 hours followed by a sustained MH release stage beyond 12 hours. MH release was 49.722 percent for MH/PCL (E) fibrous scaffolds and 83.96 percent for MH/PCL (B) fibrous scaffolds after 12 hours, figure (14, a). Over two days, the total MH release for MH/PCL (E) fibrous scaffolds was 62.12 percent and 88.973 percent for MH/PCL (B) fibrous scaffolds. The total MH release percentage for the three weeks was 71.11 percent for MH/PCL (E) fibrous scaffolds and 93.91percent for MH/PCL (B) fibrous scaffolds, as shown in Figure (14, a). Previous research has shown that when hydrophilic drugs have loaded into hydrophobic polymers, they migrate to the fiber surface [25]. During blend electrospinning, a significant quantity of hydrophilic drugs may be trapped on the fiber's surface, resulting in a high burst release in emulsion electrospinning.

The water phase had dropped into the polymer-surfactant solution, and the drug was encased by surfactants and polymer, resulting in a core-shell structure [26]. The result is attributed to a small fiber diameter indicating a greater surface area to volume ratio, increasing water penetration and exposure, resulting in significant degradation rates. Lee et al. discovered that the release pattern of PDGF-BB from heparin-attached PCL/gelatin scaffolds was dependent on fiber diameter, with smaller diameter fibers exhibiting quicker release [27]. Consequently, 5% w/v PCL scaffold has a smaller fiber diameter, and 15% w/v PCL scaffold has a thicker fiber, which may explain the MH release behavior of different scaffold concentrations.

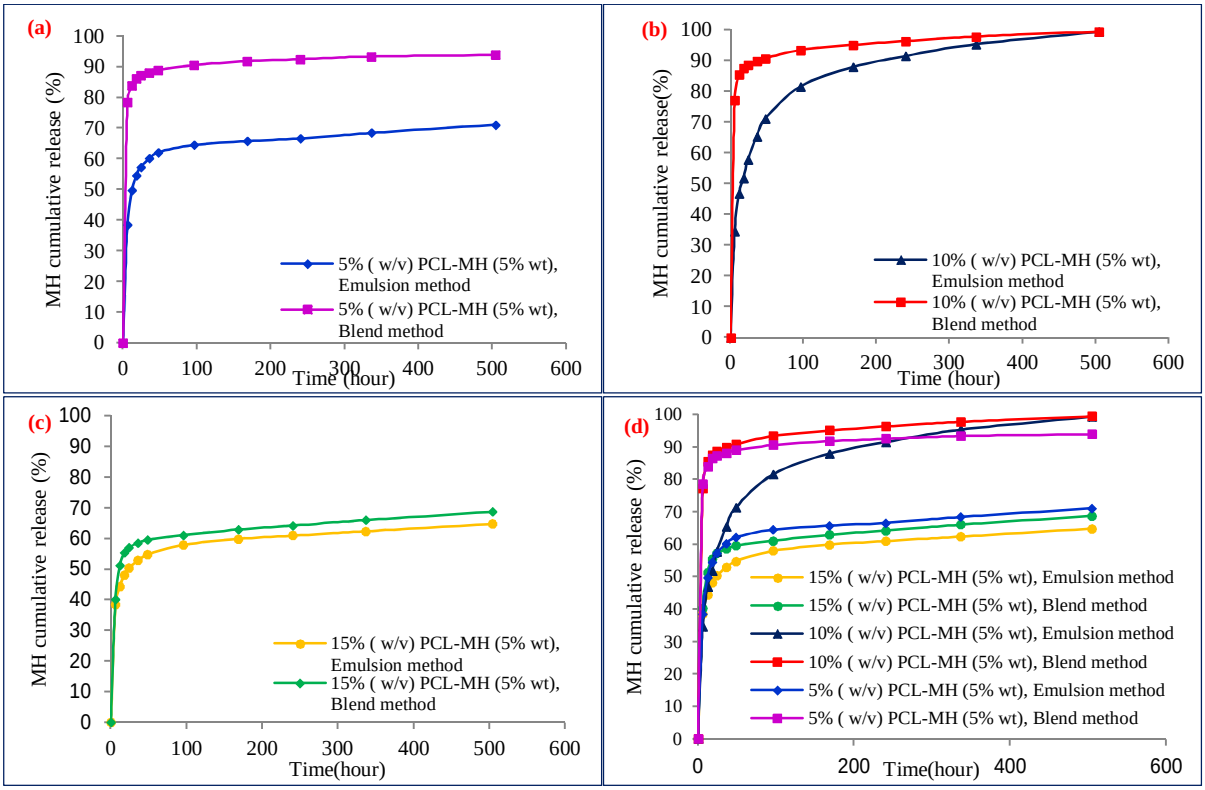

Figure 14: (a) MH release profile of 5 % (w/v) PCL-MH(5%), (b) MH release profile of 10 % (w/v)PCL-MH(5%), (c) MH release profile of 15 % (w/v)PCL-MH(5%), and (d) Comparative release profile of MH from emulsion versus blend nanofibers

4. Conclusion

Metformin hydrochloride-loaded nanofibers were prepared from PCL as the polymer matrix through an emulsion and blend electrospinning technique. The wettability result showed that the emulsion electrospinning method might help improve the hydrophilicity of hydrophobic nanofibers substrates. Compared to blend electrospun nanofibers, emulsion electrospun nanofibers reduced the initial burst release and continuously released drugs. Furthermore, the MH–15 % (w/v) PCL emulsion electrospun nanofibers demonstrated a lower and slower drug release rate than (5,10) % (w/v) PCL emulsion electrospun nanofibers. This suggests that 15 % (w/v) PCL is the most suitable drug delivery matrix compared to the lower PCL concentration. On the other hand, the emulsion method scaffolds enhanced mechanical properties and hydrophilicity. Our results indicate that emulsion electrospinning technology is a promising method for producing core-shell nanofibers to design controlled-release drug delivery systems and adjust drug release rates by altering the oil and water phases.

Acknowledgment

The authors are thankful to Ms Eng. Abeer Samir Mahmoud Saleh chemical Eng. Dept. Univ. of Tech. for providing guidance in the research work.

Author Contribution

Akram R. Jabur, Emad S. Al- Hassani, Ahmed M. Al-Shammari: supervision, writing—review and editing, analyzed and interpreted the data; Contributed reagents, materials, analysis tools or data, project administration Saja A. Moosa: Conceptualization and methodology the experiments; Performed the experiments; Analyzed and interpreted the data; Contributed reagents, materials, analysis tools or data;data curation, writing—original draft preparation Wrote the paper. All authors have read and agreed to the published version of the manuscript.

Funding

"This research received no external funding"

Conflicts of Interest

"The authors declare no conflict of interest"

References

[1] X. Feng, L. Jiannan, X. Zhang, T. Liu, J. Ding, X. Chen, Electrospun polymer micro/nanofibers as pharmaceutical repositories for healthcare, J. Control. Release, 302 (2019) 19-41. https://doi.org/10.1016/j.jconrel.2019.03.020

[2] L. Shang; Y. Yu, Y. Liu, Z. Chen, T. Kong, Y. Zhao, Spinning and Applications of Bioinspired Fiber Systems, ACS Nano, 13 (2019) 2749–2772. https://doi.org/10.1021/acsnano.8b09651

[3] S. Kajdič, O. Planinšek, M. Gašperlin, P. Kocbek, Electrospun nanofibers for customized drug-delivery systems, J. Drug Deliv. Sci. Technol., 51(2019) 672–681. https://doi.org/10.1016/j.jddst.2019.03.038

[4] A. R. Jabur , Multiwall Carbon Nanotube / Polyvinyl Alcohol Nanofibers Film, Electrical Conductivity Improvement, Eng. Technol. J., 38 (2020) 430-438. https://doi.org/10.30684/etj.v38i3A.530

[5] C. E. Ayres, B. S.r Jha, S. A. Sell, G. L. Bowlin, D. G. Simpson, Nanotechnology in the design of soft tissue scaffolds: innovations in structure and function, Wiley Interdisciplinary Reviews: Nanomedicine and Nanobiotechnology, 2 (2010) 20–34. https://doi.org/10.1002/wnan.55

[6] S. A. Moosa, A. R. Jabur, E. S. Al- Hassani, Preparation and Physical Properties of PCL-Metoprolol Tartrate Electrospun Nanofibers as Drug Delivery System, Key Eng. Mater. J., 886 (2021)183-188. https://doi.org/10.4028/www.scientific.net/KEM.886.183

[7] Y. Yang, X. H. Li, M. B. Qi, S. B. Zhou, J. Weng, Release pattern and structural integrity of lysozyme encapsulated in core-sheath structured poly(DL-lactide) ultrafine fibers prepared by emulsion electrospinning, Eur. J. Pharm. Biopharm., 69 (2008)106–116. https://doi.org/10.1016/j.ejpb.2007.10.016

[8] A. R. Jabur, L. K. Abbas, S. M. Muhi Aldain, Effects of Ambient Temperature and Needle to Collector Distance on PVA Nanofibers Diameter Obtained From Electrospinning Technique, Eng. Technol. J., 35(2017) 340-347. https://doi.org/10.30684/etj.35.4A.5

[9] J. Hu, M. P. Prabhakaran, X. Ding, S. Ramakrishna, emulsion electrospinning of polycaprolactone: influence of the surfactant type towards the scaffolds properties, J. Biomater. Sci. Polym. Ed., 26 (2014) 57-75. https://doi.org/10.1080/09205063.2014.982241

[10] D. Narasimha rao, M. Prasada rao, J. Naga Hussain, S. Lakshmi Sumanoja , V. Rajeswara rao, Method development and validation of forced degradation studies of metformin hydrochloride by using UV spectroscopy, Int. J. Pharm. Chem. Biol. Sci., 35 (2013) 546-553.

[11] H. Ruchi Majithia, Dr. Akruti Khodadiya, and B.Vaibhav Patel, Spectrophotometric method development and validation for simultaneous estimation of Anagliptin and Metformin HCl BY Q - Absorption ratio method in synthetic mixture, Heliyon , 6 (2020) 1-7. https://doi.org/10.1016/j.heliyon.2020.e03855

[12] J. Hu, M. P. Prabhakaran, X. Ding, S. Ramakrishna, Emulsion electrospinning of polycaprolactone: influence of surfactant type towards the scaffold properties, Biomater. Sci., Polym. Ed. J., 26 (2014) 57–75. https://doi.org/10.1080/09205063.2014.982241

[13] M.Pezeshki-Modaress, M. Zandi ,S. Rajabi,Tailoring the gelatin/chitosan electrospun scaffold for application in skin tissue engineering: an in vitro study, Prog. Biomater., 7 (2018) 207–218. https://doi.org/10.1007/s40204-018-0094-1

[14] J. Hu, M. P. Prabhakaran, L. T., X. Ding, S. Ramakrishna, Drug-loaded emulsion electrospun Nanofibers: characterization, drug release and in vitro biocompatibility, RSC Adv. J., 5 (2015) 100256–100267. https://doi.org/10.1039/C5RA18535A

[15] M. Alves da Silva, A. Crawford, J. Mundy, A. Martins, J. V. Arau' jo, P. V. Hatton, R. L. Reis, N. M. Neves, Evaluation of extracellular matrix formation in polycaprolactone and starch- compounded polycaprolactone nanofiber meshes when seeded with bovine articular chondrocytes, Tissue Eng. Part A, 15 (2008) 1-9. https://doi.org/10.1089/ten.tea.2007.0327

[16] L. Du, H. Xu, Y. Zhang, F. Zou, Electrospinning of Polycaprolactone Nano-fibers with DMF Additive: The Effect of Solvent Proprieties on Jet Perturbation and Fiber Morphologies, Fibers Polym., 17(2016) 751-759. https://doi.org/10.1007/s12221-016-6045-3

[17] A. R. Jabur, L. K. Abbas, S. A. Moosa, Fabrication of Electrospun Chitosan/Nylon 6 Nanofibrous Membrane toward Metal Ions Removal and Antibacterial Effect, Adv. Mater. Sci. Eng. , 2016 (2016) 10. https://doi.org/10.1155/2016/5810216

[18] N. Kulpreechanan, T. Bunaprasert, R. Rangkupan, Electrospinning of Polycaprolactone in Dichloromethane/ Dimethylformamide Solvent System, Adv.Ma. Res., 849 (2014) 337-342. https://doi.org/10.4028/www.scientific.net/AMR.849.337

[19] X.Qin, D. Wu, Effect of different solvents on poly(caprolactone) (PCL) electrospun nonwoven membranes, J .Therm. Anal. Calorim., 107 (2012)1007–1013. https://doi.org/10.1007/s10973-011-1640-4

[20] S. Gunasekaran , R. K. Natarajan, V Renganayaki, S. Natarajan, Vibrational spectra and thermodynamic analysis of metformin, Indian J. Pure Appl. Phys., 44(2006) 495-500.

[21] V. Milleret, Th. Hefti, H. Hall, V. Vogel, D. Eberli, Influence of fiber diameter and surface roughness of electrospun vascular grafts on blood activation, Acta Biomater., 8 (2012) 4349-4356. https://doi.org/10.1016/j.actbio.2012.07.032

[22] X. Q. Li, Y. Su, X. Zhou , X. M. Mo, Distribution of sorbitan monooleate in poly(1-lactide –co-e-caprolactone) nanofibers from emulsion electrospinning, Colloids Surf. B: Biointerfaces, 69 (2009) 221–224. https://doi.org/10.1016/j.colsurfb.2008.11.031

[23] Shing- Chung Wong, Avinash Baji, Siwei Leng, Effect of fiber diameter on the tensile properties of electrospun poly (ε-caprolactone), Polymer, 49 (2008) 4713-4722. https://doi.org/10.1016/j.polymer.2008.08.022

[24] Y. Ankamma Chowdary, R. Raparla, M. Madhuri , Formulation and Evaluation of Multilayered Tablets of Pioglitazone Hydrochloride and Metformin Hydrochloride, J. Pharm., 2014 (2014) 1-14. https://doi.org/10.1155/2014/848243

[25] E.R. Kenawy, F. I. Abdel-Hay, M. H. El-Newehy, G. E. Wnek, Processing of polymer Nanofibers through electrospinning as drug delivery systems, Mater. Chem. Phys . J., 113 (2009) 296–302. https://doi.org/10.1007/978-1-4020-9491-0_19

[26] A. Szentivanyi, T. Chakradeo, H. Zernetsch , B. Glasmacher, Electrospun cellular microenvironments: Understanding controlled release and scaffold structure, Adv. Drug Deliv Rev. J., 63 (2011) 209–220. https://doi.org/10.1016/j.addr.2010.12.002

[27] J. Lee, J. J. Yoo, A. Atala, S. J. Lee, The effect of controlled release of PDGF-BB from heparin-conjugated electrospun PCL/gelatin scaffolds on cellular bioactivity and infiltration, Biomaterials , 33 (2012) 6709-6720. https://doi.org/10.1016/j.biomaterials.2012.06.017